Received: 8 March 2024 | *Revised:* 23 April 2024 | *Accepted:* 25 April 2024
DOI: 10.37917/ijeee.22.1.13 *Vol. 22 | Issue 1 | June 2026*

Iraqi Journal for Electrical and Electronic Engineering
Original Article

Open Access
IJEEE University of Basrah College of Engineering

A LVRT Control Strategy of PMSG Based Wind Farm Under Different Grid Faults

Ahmed Muthanna Nori*, Ali Kadhim Abdulabbas
Electrical Engineering Department, University of Basrah, Basrah, Iraq

Correspondance
*Ahmed Muthanna Nori
Electrical Engineering Department
University of Basrah, Basrah, Iraq
Email:eng.ahmed.m@uobasrah.edu.iq

Abstract
Wind Energy Conversion Systems (WECSs) have experienced significant growth in recent years.Among various types of generators employed in WECSs,Permanent Magnet Synchronous Generators (PMSGs) are an attractive choice among the wide variety of wind generators due to several advantages.The growing penetration of PMSG-based WEGSs into the worldwide electrical grid raises the concern that the failure of wind turbine generators may potentially result in the collapse of the system.This prompted several countries to adopt the Low-Voltage Ride-Through (LVRT) for wind farms.LVRT is the capability to maintain the connection between the wind farm and the grid during certain periods of voltage sag.This paper presents an efficient LVRT control strategy for a 12.0MW (6*2MW) grid-connected PMSG-based Wind Farm (PMSG-WF).The proposed strategy aims to enhance the power quality and amount of injected power to achieve the grid code requirements by integrating a Braking Chopper (BC) and a Dynamic Voltage Restorer (DVR) with the conventional structure of PMSG-WF. The detailed mathematical models for a wind turbine, PMSG, power converters, DVR system, and grid model are utilized to analyze the dynamic behavior and operation of PMSG-WF.For DVR, a PI controller is used for voltage sag mitigation to inject reactive power during grid faults, while a hysteresis controller-based BC system is utilized to keep DC-link voltage within its permissible limits.The proposed system is exposed to three scenarios of symmetrical and asymmetrical grid fault conditions (single-phase, two-phase, and three-phase faults) at the point of common coupling to evaluate its dynamic response.MATLAB/SIMULINK environment is used to validate the effectiveness of the proposed strategy during the studied scenarios.The results show the superiority of DVR in improving the voltage stability of PMSG-WF and maintaining the uninterrupted operation of the grid during different grid faults.

Keywords
WECS, PMSG, Wind Farm, Low Fault Ride-Through, Grid Fault, Dynamic Voltage Restorer, Breaking Chopper.

I. Introduction

The integration of Renewable Energy Systems (RESs) has increased rapidly in recent years, and the decarbonized global energy system is expected to save approximately $12 trillion by the middle of this century.The RESs, particularly wind farms, will help to increase worldwide demand for green energy by reducing the cost of manufacturing, distribution, and losses, also permitting greater renewable energy generation.As a consequence, the researchers concentrated their attention on using wind energy [1].With the increasing integration of wind power into the electrical infrastructure,the impact on the dependability and stability of power systems emerges as an important worldwide issue. In response to such situations,grid operators have suggested grid codes to standardize the characteristics of the Wind Energy Conversion Systems (WECS).One of the most important issues related to grid codes is Low-Voltage Ride-Through (LVRT),states that in the event of a grid fault, the WECS must maintain connectivity and provide reactive current to support the grid [2].This LVRT is a significant concern in wind turbine systems.In this

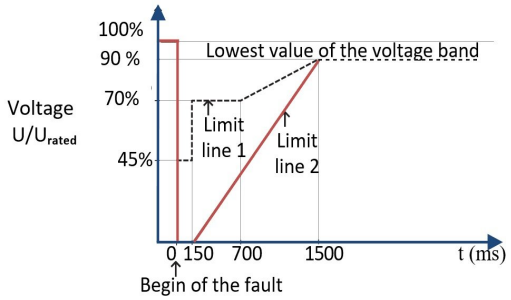

Fig. 1. Limit curves of the voltage that permit disconnecting the generator

context, network codes for grid connection establish appropriate voltage ranges that serve as a guide for wind turbine disconnection,as shown in the LVRT voltage-time profiles of Fig.1.The connection should be kept when the grid voltage exceeds Limit line 1, if the voltage drops under limit Line 2 the system should be disconnected [3].
Furthermore, reactive power must be provided by wind farm to the grid dependent on the depth of voltage sag to support the recovery of grid voltage. So, the required minimum reactive current during a voltage sag can be calculated,as illustrated in Fig.2.Accordingly, the reactive and active powers have to change to correspond with the reactive current-voltage profile and also with the voltage-time profile [4].

Currently, there are two predominant variable speed Wind Turbine Generators (WTG) in wind energy technology: the Doubly-Fed Induction Generator (DFIG) and the Permanent Magnet Synchronous Generator (PMSG) [5]. Recently, significant attention is being given to PMSG due to its superior characteristics in comparison to other prevailing alternatives, including maximum power extraction, high efficiency, reliability, high torque, and no gearbox. These merits are sufficient to compel the wind market to shift its focus towards the PMSG industry [6]. DFIG uses partial Back-to-Back Converter (BTBC) and relies on a gearbox for its operation. In

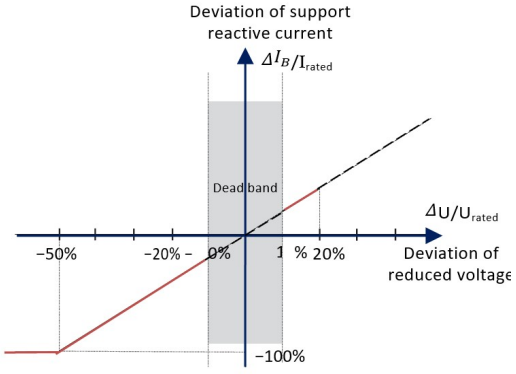

Fig. 2. Reactive current demand

contrast,PMSG does not need a gearbox and employs full-scale BTBC. Protecting full-scale BTBC is crucial and essential because they are more expensive and operate at a higher efficiency than their partial counterparts [7]. Even though DFIG has a lower Fault Ride-Through Capability (FRTC) than PMSG, it remains revolutionary for enhancing FRTC of PMSG. This is because the accumulated surplus power in the DC link during voltage swell and sag can cause overvoltage, potentially leading to the tripping of the entire wind system [8]. Many methods are tested with their control strategies during asymmetrical and symmetrical faults to attain FRTC, even if the system's voltage is zero. They are presented and researched to address this issue; however, these systems have advantages and, of course, limitations [9]. This paper proposes a novel FRT configuration for maintaining PMSG-based Wind Farm (PMSG-WF) grid voltage to pre-fault levels during severe voltage dips.

Faults may result due to several causes, such as short circuits, the startup of induction machines, the connecting of capacitive loads, and so forth. The fault types that occur in the electrical power system are commonly categorised as either unsymmetrical (e.g., Single line to ground fault (SLG fault); Line to line fault (LL fault); and Double line to ground (LLG fault)) or symmetrical (e.g., Three line to ground fault 3 LG), as seen in Table 1. Table 1 indicates that SLG has the largest occurrence rate, although it has a far lower influence on the system. In contrast, the occurrence of 3LG is rare, although its effect on the system is far more severe [1]. To guarantee safe and dependable operation, FRTC has emerged as the most extensively utilized grid connection standard for PMSWG worldwide. The intrinsic instability and intermittency of the wind system, along with the increasingly weak grid connectivity, provide a considerable challenge and relevance to the FRTC subject [10].

To accomplish FRTC, the wind system has to withstand faults and stay connected to the power grid so that both frequency and voltage remain unchanged after and before the fault. Many research have been conducted to overcome problems in the PMSG Wind Turbine (PMSG-WT) structure and increase FRTC during different fault conditions [11]. The developed strategies split into two main groups. The first is a software solution that includes Pitch Angle Control (PAC) method and a modified control technique method applied on converters in the occurrence of a failure. However, this technique is only suitable for moderate voltage changes. Another type of solution is hardware, involving energy storage, Braking Chopper (BC), FACTS, Superconducting Fault Current Limiters (SFCL), and Series Dynamic Braking Resistors (SDBR) [12].

The BC system was suggested to be connected in parallel with the DC-link to waste surplus energy and keep the

TABLE I.
TYPE OF FAULTS AND THEIR % HAPPENS

Fault Type	Occurrence Percentage%
Single line to ground	70-85
Double line	15-8
Double line to ground	10-4
Three line to ground	5-3

DC-link voltage within the required range during grid disturbances.The BC consists of a high-power resistor and a series of IGBT switches, which offer low cost and a simple control structure [13].According to [14],the Dynamic Voltage Restorer (DVR) can increase the FRTC of the PMSG by injecting the desired voltage at the wind farm terminals. Its components include a Voltage Source Converter(VSC) including DC voltage with an inverter,a harmonic filter as LC filter, and a coupling transformer.The DVR system's goal is to supply voltage to generate the required grid voltage.Thus, the grid terminal maintains its rated voltage during normal and fault conditions.As a consequence, even if there are grid failures, no transients of PMSG current and power happen.In this general context, and because the several advantages of using BC and DVR, the proposed idea in this research paper is to integrate a BC and a DVR with the PMSG-WF structure and benefit from their abilities to compensate for the fault effect on the considered structure by maintaining the PMSG-WF connected to the grid during different faults. The present paper is organized as follows: Section II. presents a brief description of the proposed system. In section III. , the modeling of the proposed configuration for a grid-connected PMSG based wind farm is introduced.Section IV. presents the control strategy of the PMSG-based wind turbine system, BC, and DVR. The simulation results and discussion under various grid faults are shown in section V. . Finally, concluding remarks are presented in Section VI. .

II. BASIC DESCRIPTION OF THE PROPOSED SYSTEM

A diagram of the PMSG-based wind farm described in this paper is shown in Fig.3.It comprises of 6 units of 2 MW variable-speed PMSG-based wind turbine generators associated to a BC and a DVR.The wind farm is structured as an underground electricity cable-connected internal network.Each WTG is filtered by an LC filter and equipped with 0.69/25 kV step-up transformer.The complete wind farm is directly interconnected to the electrical grid via the Point of Common Coupling (PCC).A traditional Single-Machine Infinite Bus type (SMIB) system is utilized to represent the utility electric system. These components are interconnected via a 30 km tie-line.It operates at 25 kV on the grid side and 120 kV/50 Hz on the bulk power system side, and uses a Thevenin equivalent to implement a 2500 MVA short circuit power level infinite bus. To reduce DC-link voltage spikes caused by unbalanced energy, the BC is linked to the DC-link of each individual WTG. The DVR is a series connected power electronics based custom power device between the PCC and the utility grid which is capable of injecting an appropriate voltage in the same phase as that of network voltage at PCC . The proposed strategy aims to regulate the DC-link capacitor and ensure voltage stability at PCC to enhance power quality and improve the FRTC of the PMSG-WF.During a fault, the DVR gets activated and injects synchronized voltage with the network voltage (V_g) to compensate for the voltage dips utilizing power from the Direct Current (DC) power supply in order to restore the amplitude of the PCC voltage (V_{pcc}) to its rated value.Additionally,the BC is responsible for absorbing excess power (P_{bc}) resulting from the difference between the generated power(P_g) and the grid power(P_{grid}).The excess power is dissipated in the resistor of BC, which is controlled using a duty ratio (D) to keep the DC-link voltage within an acceptable range.

III. WIND ENERGY CONVERSION SYSTEM MODELING

In this section, detailed models for each component of the proposed system are presented separately, consisting of the wind turbine, PMSG, BTBC, the DVR system, and the electric utility grid as shown in Fig.3. The wind turbine generator considered in this paper employs PMSG directly coupled to the wind turbine (without gearbox) and connected to the LC filter and 0.69/25 kV step-up transformer through BTBC which consists of a pair of converters, Machine-Side Converter (MSC) and Grid-Side Converter (GSC). Between the two converters a combination of DC-link capacitor with BC.

A. Wind Turbine Model:

The wind turbine converts wind energy into mechanical energy. The mechanical power output of the wind turbine P_w is calculated as $P_w = 0.5\rho\ \mathrm{A}V_w^3$, where ρ, A are the air density and the area swept by the blades,respectively;V_w is the wind speed.As per Betz's law, the actual mechanical power P_m can be extracted from the wind power, which is directly proportional to the coefficient of performance C_p, i.e., $P_m = C_p\ P_w$, where C_p is a function of β(pitch angle) and λ (tip-speed ratio). The power output from the wind turbine generator can be represented by equation (1) [15] .

$$P_m = 0.5\rho A C_P(\lambda,\beta)V_w^3 \tag{1}$$

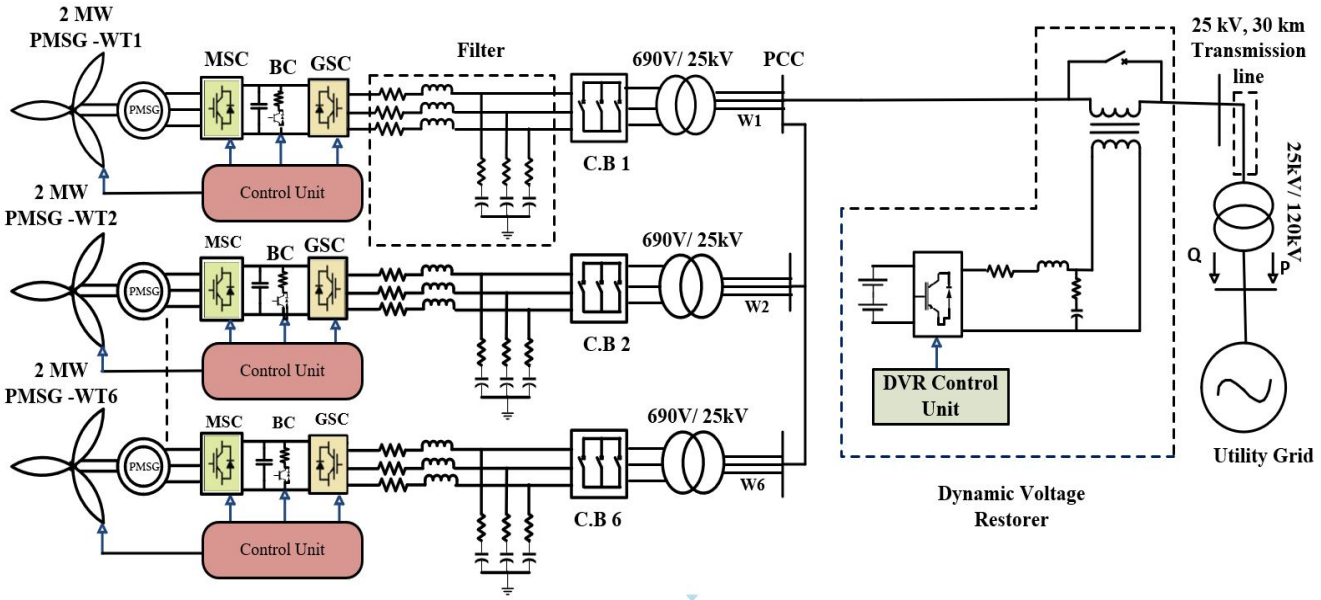

Fig. 3. Power system diagram for the proposed circuit

$$\lambda = \frac{\omega_R R}{v_w} \tag{2}$$

The equation representing the tip speed ratio is equation (2): where ω_R and R are the turbine angular speed and the radius of the rotating turbine blade, respectively. The coefficient of performance C_P is given by equation (3) [15].

$$C_P(\lambda,\beta) = 0.5176(\frac{116}{\lambda_i} - 0.4\beta - 5)e^{\frac{-21}{\lambda_i}} + 0.0068\lambda \tag{3}$$

where λ_i is defined by

$$\frac{1}{\lambda_i} = \frac{1}{\lambda_i + 0.08} - \frac{0.035}{\beta^3 + 1} \tag{4}$$

The mechanical torque T_m can be calculated by dividing the mechanical power P_m by the angular velocity ω_R.Wind turbine achieves maximum value of power coefficient C_{pmax} at optimal tip speed ratio λ_{opt} .For $\beta = 0^0$ the obtained value of C_{pmax} is 0.45 and λ_{opt} is 10.54, where the wind turbine captures the maximum power from the wind [16].

B. PMSG Model:

PMSG converts the mechanical form of wind energy into electrical energy. The mathematical representation of a PMSG can be described in the direct axis frame (d-axes) and quadrature axis frame (q-axes) using an equivalent circuit given by equations (5) and (6) [17].

$$u_{sd} = R_s i_{sd} + L_s \frac{di_{sd}}{dt} - \omega_e L_s i_{sq} \tag{5}$$

$$u_{sq} = R_s i_{sq} + L_s \frac{di_{sq}}{dt} + \omega_e L_s i_{sd} + \omega_e \psi_m \tag{6}$$

where, u_{sd} and u_{sq} are the stator voltages; i_{sd} and i_{sq} are the stator currents;ω_e is the angular electrical rotating speed of the generator ; L_s is the stator inductance of the PMSG;R_s is the stator resistance of the PMSG; and ψ_m is the permanent magnet flux linkage.The electromagnetic torque produced by the PMSG can be expressed by equation (7) [17].

$$T_e = \frac{3}{2} p_n [(L_d - L_q) i_{sd} i_{sq} + \psi_m i_{sq}] \tag{7}$$

where p_n is the number of pole pairs of the PMSG;L_d and L_q are the stator inductance in the d-axis and q-axis, respectively.

C. BTBC Model:

The configuration of BTBC is shown in Fig.3, which is used to control the WTG based on PMSG. Both converters in BTBC are built on the three-phase two-level voltage source converter (VSC), which consists of two insulated-gate bipolar transistors (IGBTs) in each phase.This allows power to flow bidirectionally between the DC-link and PCC via a step-up transformer. The DC-link acts as an energy buffer between the MSC and GSC, enabling independent control of the converters on either side. The BTBC model comprises an MSC model as a rectifier and a GSC model as an inverter. Two converters are connected via a DC-link [3], as seen in Fig.4.

1) MSC Model:

The schematic diagram of the rectifier connecting the wind turbine generator to the DC-link is depicted in Fig.4.The math-

ematical model for the rectifier is written as follows [18].

$$\begin{bmatrix} u_{sa} \\ u_{sa} \\ u_{sa} \end{bmatrix} = \frac{1}{3} \begin{bmatrix} 2 & -1 & -1 \\ -1 & 2 & -1 \\ -1 & -1 & 2 \end{bmatrix} \begin{bmatrix} S_a \\ S_a \\ S_a \end{bmatrix} U_{dc} \tag{8}$$

where u_{sa},u_{sb}, u_{sc} are the stator phase voltages (a, b, and c);U_{dc} is the DC-link voltage.The switching phase states (a, b and c) are S_a , S_b, S_c.Then S_k (k = a, b, c) is represented as:
S_k= 1 (Upper switch on, lower switch off),
S_k=0 (Upper switch off, lower switch on).
The upper switches are T_1, T_3, T_5, and the lower switches are T_4, T_6, T_2 with respect to phase a, b and c.
The stator voltages in the rotating dq-axis can be obtained from the transformation of three-phase stator voltages in the abc frame by [3].

$$\begin{bmatrix} u_{sa} \\ u_{sa} \\ u_{sa} \end{bmatrix} = \begin{bmatrix} \cos\theta & -\sin\theta & 1 \\ \cos(\theta - \frac{2\pi}{3}) & -\sin(\theta - \frac{2\pi}{3}) & 1 \\ \cos(\theta + \frac{2\pi}{3}) & -\sin(\theta + \frac{2\pi}{3}) & 1 \end{bmatrix} \begin{bmatrix} u_{ds} \\ u_{qs} \\ u_0 \end{bmatrix} \tag{9}$$

where u_0 represents the zero-sequence voltage.

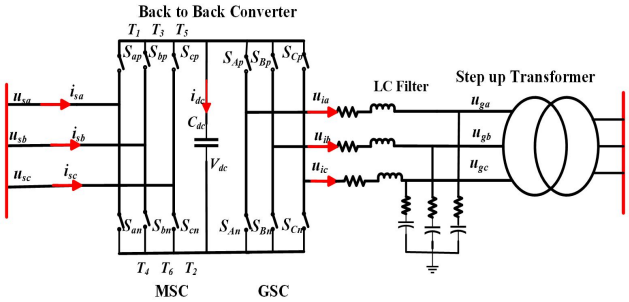

Fig. 4. Model of the MSC and GSC

2) DC-Link Model:

For proper working of MSC and GSC, it is necessary to regulate the voltage across the DC-link even during grid fault case.The DC-link voltage can be described according to power relationship by Fig.(10) [19]:

$$CU_{dc}\frac{dU_{dc}}{dt} = P_{gen} - P_g = \Delta P \tag{10}$$

where, C is the dc-link capacitance. P_{gen}, P_g, and Δ P are the generator power,the grid power,and the power difference between them, respectively.During normal grid operation, the generated power and the grid power are equal, resulting in no change in power (Δ P = 0).

3) GSC Model:

The PMSG wind turbine is tied to the power grid via the GSC as illustrated in Fig.4. The GSC is responsible for regulating the DC-link voltage and transfers the power fed from the MSC to the grid.The three-phase outputs of the GSC are linked to the grid at the PCC through interfaced passive LC filter and step-up transformer, where the filter and transformer are represented by inductors L_g and resistors R_g. The dynamic model of the GSC can be described as follows [20].

$$u_{gd} = u_{id} - R_g i_{gd} - L_g\frac{di_{gd}}{dt} + \omega_g L_g i_{gq} \tag{11}$$

$$u_{gq} = u_{iq} - R_g i_{gq} - L_g\frac{di_{gq}}{dt} - \omega_g L_g i_{gd} \tag{12}$$

where, u_{gd} and u_{gq} are the dq-components of grid voltage;i_{gd} and i_{gq} are the dq-components of grid current;and u_{id} and u_{iq} represent the GSC output voltages in dq frame and ω_g is the grid voltage angular frequency. It is assumed that the dq-axis rotating reference frame is aligned with the grid voltage. The active and reactive power transmitted to the grid are given by the following quations [20].

$$P = \frac{3}{2}u_{gd}i_{gd} \tag{13}$$

$$Q = \frac{3}{2}u_{gq}i_{gq} \tag{14}$$

So, the reactive power and active power transmitted to the power grid can be regulated by i_{gq} and i_{gd} which are also known as reactive and active current, respectively.

D. DVR Model:

The DVR in the proposed system consists of an energy storage unit, VSC, LC filter,and a series-connected injection transform.It is coupled in series with the PMSG-WF terminal's power line through 3 single-phase ideal transformers to rapidly compensate for voltage sags .The VSC converts the voltage across the storage device into a set of three phase sinusoidal output voltages at desired magnitude, phase angle,and constant frequency.The LC filter in the DVR is needed to reduce the switching harmonics generated by the PWM VSC.

1) DVR Side Converter:

Fig.5(a) shows the standard topology of a two-level VSC, where, i_{fabc} and u_{fabc} represent the three-phase currents and voltages on the AC side. To simplify the analysis, the two-level VSC is represented by an average-value model, as illustrated in Fig.5(b).This model can considerably enhance simulation speed in addition to being a very similar steady state and dynamics with the first model.The components of the three-phase voltages are u_{fa}, u_{fb}, and u_{fc} as seen in Fig.5(b) produced by the VSC, and are represented as function modulation indices m_a, m_b, and m_c of the ac voltage as follows [21].

$$u_{fi} = 0.5 m_i U_B, i = a, b, c \tag{15}$$

Assuming the DVR side converter is lossless, then the current can be written as follows.

$$i_B = 0.5\sum_{i=a}^{c} m_i i_{fi} \tag{16}$$

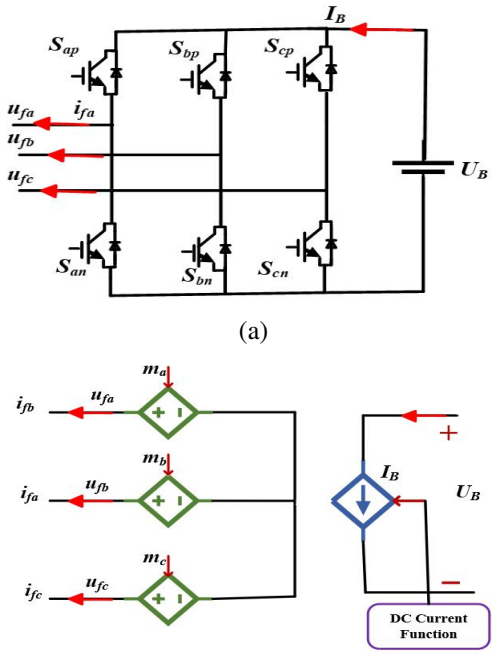

Fig. 5. Two-level VSC topology. (a) Configuration of the standard model. (b) Configuration of the Average-value model

2) LC Harmonic Filter:

The LC harmonic filter model can be represented by the relationship between its voltages and currents input and output as follows [21].

$$u_{fi} = L_f \frac{d_{if}}{dt} + u_c \tag{17}$$

$$i_{fi} = C_f \frac{d_{vf}}{dt} + i_c \tag{18}$$

where C_f and L_f are the parameters of filter. $u_f(i_f)$ are the voltage (current) produced by the DVR Side converter, and $u_c(i_c)$ are the voltage (current) for compensating.

3) Single phase Transformers:

The three single-phase transformers of the DVR are presumed to be ideal. Then, the voltages and currents of the primary and secondary sides of each single-phase transformer are determined by [21]:

$$u_{ci} = u_{pmsg} - u_g \tag{19}$$

$$i_{ci} = i_g \tag{20}$$

where the subscript *pmsg* refers to PMSG, c is DVR compensation, and g is the utility grid.

IV. Control Scheme For Investigated System

Three power conversion systems are used according to the general topology of the PMSG-WF with DVR shown in Fig.3. These are MSC with BC, GSC, and DVR. This section will introduce the pitch angle control scheme, which is used to stabilize the PMSG output power when the wind speed exceeds its rated value. Also, the detailed control schemes for each converter will be discussed as follows:

A. Pitch Angle Control:

The pitch angle controller regulates the airflow surrounding the blade of the wind turbine, consequently managing the torque applied to the shaft of the turbine to adjust PMSG rotating speed. Wind turbine systems are adapted to speeds ranging from around 3 m/s to approximately 25 m/s, with rated power extracted at 12 to 16 m/s [22]. Fig.6 illustrates the controller of the pitch angle utilized to control the generator speed. This study concentrates on the maximum rotational speed (ω_{ref}) with a limit of 1.1 p.u. The measured rotor speed is compared to the reference value, and the result of the error enters a proportional(P) controller.Then the P controller is used to handle pitch angle reference value (β_{ref}) based on ω_{ref}. So, β_{ref} is kept constant at zero degree in conditions below the rated wind speed. When the rotational speed of PMSG exceeds the rated value due to rising wind speed, then the P controller will also increase β_{ref}, reducing the effective area of the blade to maintain the output power constant [3].

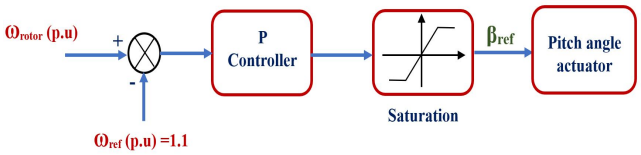

Fig. 6. Wind turbine pitch angle controller

B. MSC Control:

The main objectives of the MSC control is to achieve Maximum Power Point Tracking (MPPT) and to regulate the generator power factor.Fig.7 depicts the control block diagram of the MSC, the output of the MPPT unit serves as the torque reference value for the controller of the generator-side VSC.The torque reference obtained by a MPPT is use to create the q-axis stator current reference (I_{sqref}), which is compared with the q-axis stator current (I_{sq}) to provide the q- axis voltage signal (U_{sq}) through the PI controller. Also, to get unity power factor, the reactive power of the wind turbine is adjusted to zero (I_{sdref}=0) and compared with the d-axis stator current to get d- axis voltage signal (U_{sd}) through the PI controller. After decoupling, dq-axis voltage references, U_{sd-ref} and U_{sq-ref} are obtained, respectively.The angle θ_g derived from

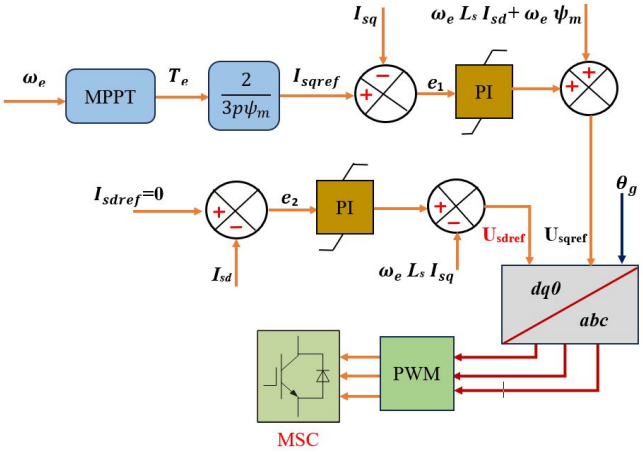

Fig. 7. Control diagram for Machine-Side Converter

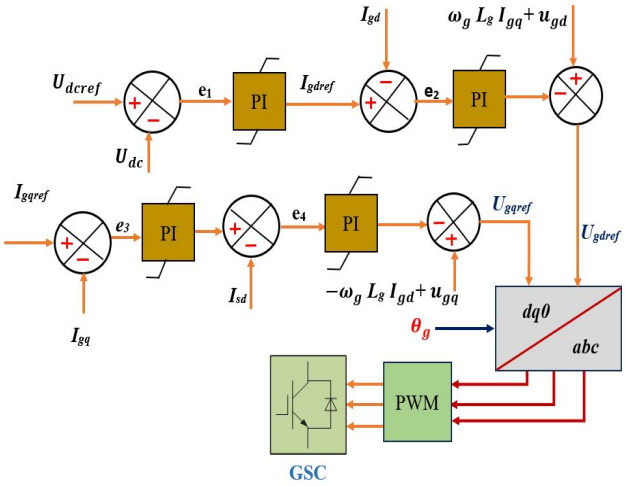

Fig. 9. Control diagram for Grid-Side Converter

the PMSG's rotating speed is used in a park transformation to generate gate signals utilizing the carrier wave of PWM operation [15].

C. DC-Link Control:

A BC is a protection device that is installed on the DC bus. It consists of a DC chopper circuit connected in series with a DC resistor, as illustrated in Fig.8.

The DC-link voltage should not exceed the rating voltage of the DC-link and converter and remain below U_{dcmax} to avoid voltage damage and stay above U_{dcmin}.While U_{dcmin} should achieve the requirement of grid-side AC voltage amplitude, i.e., $\sqrt{2}U_{line} < U_{dcmin}M_{max}$, where U_{line} and M_{max} are the magnitude of line grid voltage and maximum modulation index of the converter, respectively [23].When the DC-link voltage surpasses a specific threshold, the BC circuit conducts and discharges excess energy to maintain voltage stability.There are several control systems for braking choppers.The method of hysteresis comparison is shown in Fig.8.This method has a simple control.The duty ratio of the crowbar switch is controlled by the dead-band control to maintain the DC-link voltage. So, if the DC-link voltage exceeds the limit of 1160V during a grid voltage fault, the resistor of BC is inserted in the DC-link of the back-to-back converter to dissipate the surplus active power.

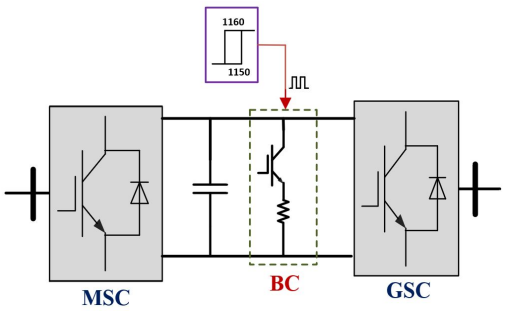

Fig. 8. BC protection for LVRT of PMSG

D. GSC Control:

The purpose of GSC control is to maintain a stable DC-link voltage.The control block diagram of the GSC is shown in Fig.**??**.During PMSG operation, the reactive current reference value is zero, allowing a greater amount of active power to be delivered to the grid.The controller of the grid side uses dual-loop PI control for q- and d-axes currents and a voltage-oriented control strategy.The active and reactive powers can be injected into the grid when the q- and d-axis currents are controlled, respectively.The maximum current capacity, I_{dmax}, is employed to generate 2 MW of active power, which is fed into the PI controller via the DC-link voltage regulator while I_{qref} is zero.A phase-locked loop (PLL) detects the park transformation angle θ_g from three-phase voltages on low-voltage side of the grid transformer . Finally, gate signals for grid-side VSC switches are created using grid-side PWM [24].

E. DVR Control:

The goal of the DVR is to quickly compensate for grid voltage disturbances and keep the sinusoidal voltage injection profile with same frequency of grid voltage [25].The DVR scheme implemented in the proposed system to mitigate the disruption is seen in Fig.10.The proposed design of the control circuitry of DVR is a combination of PLL, PI controllers, and PWM based technique,as depicted in Fig.11 .The control operation is synchronized with the supply voltages via the PLL. When fault occurs on the grid side, an error signal is generated as a result of the difference between the voltage at a PCC with the reference voltage and fed to PI controller. The PI controller minimizes the error and passes the value to the PWM generator,which in turn takes it as input and gives triggering signal as

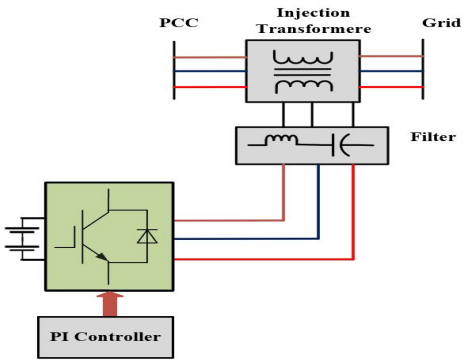

Fig. 10. DVR scheme

output to activate VSC .VCS converts the DC Energy Storage into a three-phase sinusoidal AC voltage with the required amplitude, phase, and frequency via an isolating transformer to restore the PCC voltage during grid fault.This voltage from the DVR adds up with the grid voltage at PCC, and as a result, the product becomes equal to that of the prefault voltage, consequently keeping the PCC voltage constant.

V. Simulation Results and Disscusion

The system of PMSG-WF with DVR is simulated in MATLAB/ Simulink environment as shown in Fig 12. It is a three-phase source inserted to a 12 MW wind farm based on PMSG system.

The simulink model of PMSG-WF consists of 6*2 MW PMSG-WT as illustrated in Fig.13. Each wind turbine at 0.9 power factor is injected into a 25 kV distribution system through a three phase 0.69/25kV transforme rated 4 MVA with an impedance of 5%. Fig.14 depicts the simulink model of the PMSG-based wind turbine connected to a two-level PWM back-to-back converter and an LC filter which is used to absorb high current harmonics created by the switching in the converters.The simulation model of an adapted utility grid consists of a medium transmission line of 30 km length at 25 kV that connects the wind farm to a 120 kV grid through

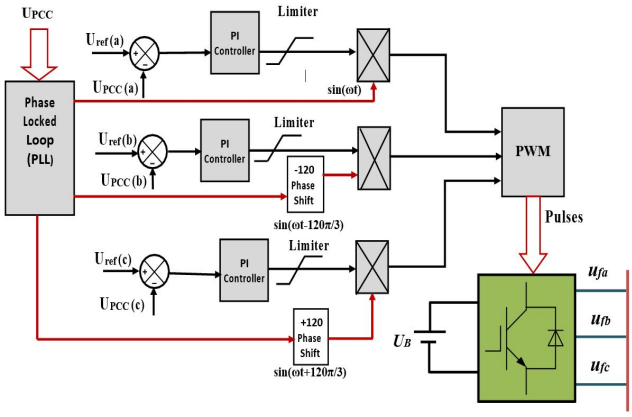

Fig. 11. Control diagram for DVR

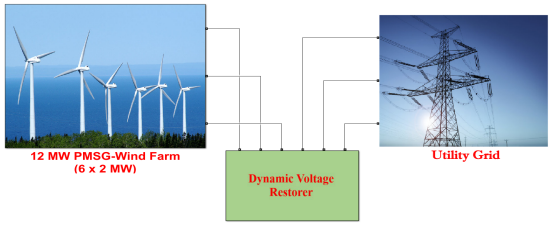

Fig. 12. The Simulink model of proposed system

a 25/120 kV transformer rated 47 MVA as shown in Fig.15. The parameters of the PMSG-WF system are listed in the Appendix.

A. *The Simulation Results of proposed system under A Symmetrical and Symmetrical Faults*

Three scenarios are simulated under voltage asymmetrical and symmetrical to evaluate the performance of the proposed system with different types of fault operation at B25kV of the utility grid to achieve FRT capability requirements as follows:

A. Single-line to ground (SLG) fault happens on system.
B. Two-line to ground (2LG) fault happens on system.
C. Three-line to ground (3LG) fault happens on system.

These tests are conducted at a wind speed of 12m/s.The results of voltage and current at PCC, reactive power, active power, generator speed, torque, and DC link voltage are exposed and

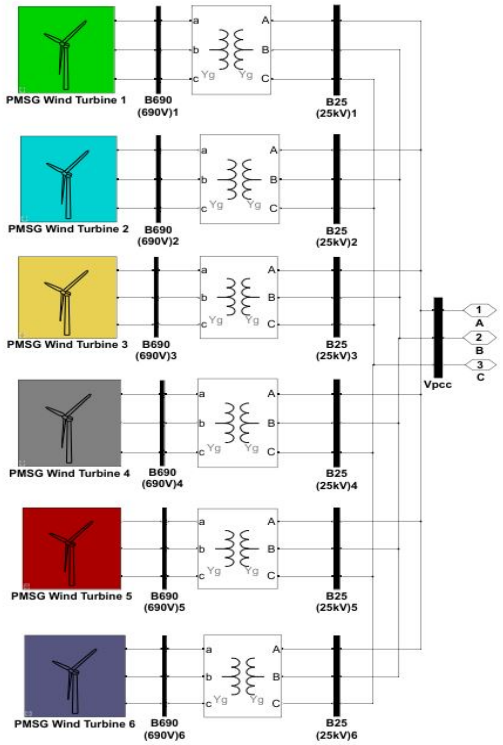

Fig. 13. Simulink model of PMSG based WF

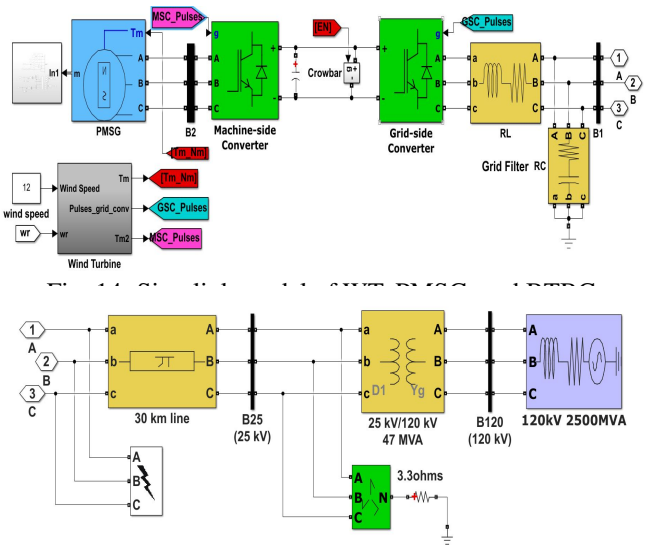

Fig. 15. Simulink model of the 120kV utility grid.

discussed in detail to show the performance of the proposed system during various fault conditions. All fault is created at t=2s and resolved at t=3s.

Test 1:The first one tests the FRT performances of PMSG-WF with DVR during SLG fault for phase A for a duration of 1s (50 cycles) between 2 s to 3 s in the utility grid, as shown in Fig.16a.The proposed strategy aims to regulate the PCC voltage by controlling the reactive power provided into the grid .When a SLG fault occurs, DVR immediately(in less than 150 ms) injects compensation voltage as illustrated in Fig.16b.As a result, the PCC voltages return to their original values, as illustrated in Fig.16c, and the PMSG-WF continues to operate normally with a constant terminal voltage.

It is obvious from Fig.17 that the grid current at PCC is perfectly limited to the rated value during fault.Since the DVR keeps a constant terminal voltage, the active power exchanged by PMSG-WF is maintained constant at its rated value of 12 MW, and the reactive power is equal to zero, with just a slight overshoot below the safety limits.Based on the aforementioned simulation results, it is needless to say that the proposed system keeps balanced three-phase values, which guarantees good power quality during the fault period. From Fig.17c, the DC-link voltage fluctuates from a reference value of 1150V to 1100 V throughout the fault occurrence and to 1135 V throughout fault resolution and rapidly recovers to its normal value,these amplitudes are considerably within its allowable margins.Thus, BC system is succeeded to remove the excess power away and maintain the dc voltage at its permissible limits.

Fig.18 illustrates the behavior of the mechanical part during SLG fault where the PMSG speed is quite immune to disturbances, while the electromagnetic torque graph shows

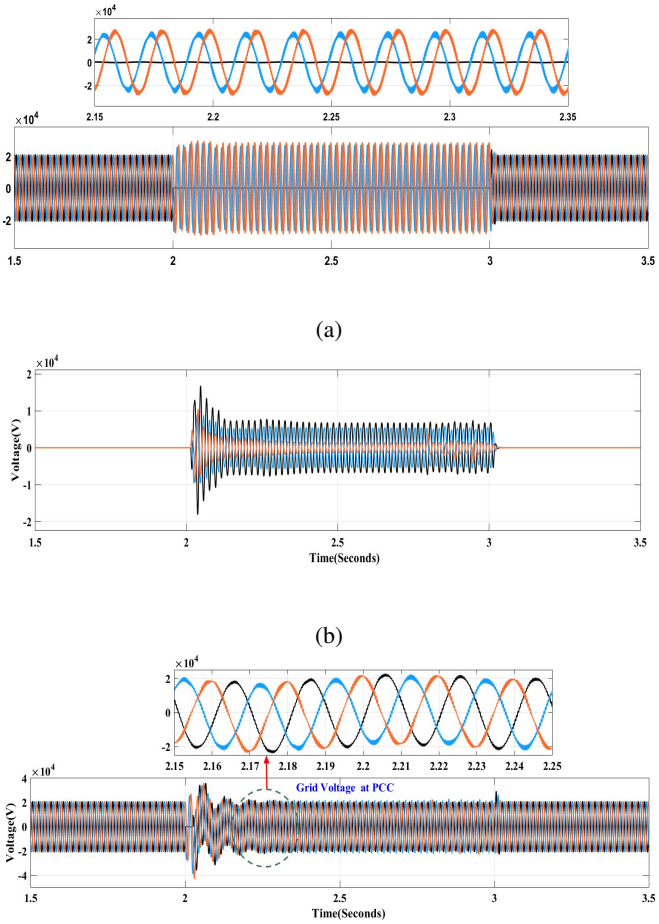

Fig. 16. (Asymmetrical grid fault SLG fault. (a) Grid voltage at B25 kV. (b) DVR compensation voltage. (c) PCC Voltage.

no oscillations during the appearance and clearance of the fault.

Test 2:In this test ,the system performance has been examined for a 2 LG fault occurring at t=2 for 1s in phases A and B in the utility grid.DVR is automatically connected at the PCC, and delivers the the necessary voltage to maintain PCC voltage in balance. Fig.19a displays the grid voltage with a 2 LG fault. The DVR quickly injects the compensation voltage as depicted in Fig.19b to rebuild the voltage at PCC. Fig.19c shows the PCC voltage after compensation.

The grid current at PCC is unchanged as shown in Fig.20a.The WF generators maintain their output of 12MW of active power, while the reactive power remains at zero, as it was before the disturbance occurred, as shown in Fig.20b.In Fig.20c, the voltage of the DC link remains constant.

Fig.21a and Fig.21b illustrate the behavior of the mechanical

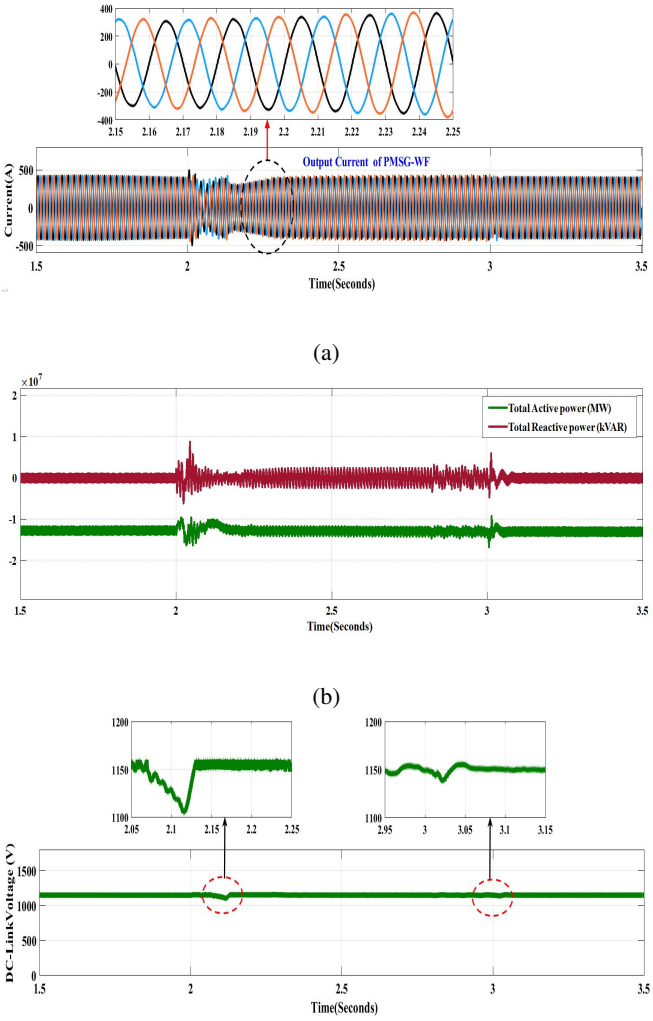

Fig. 17. (a) Output current of PMSG-WF (b) Active power and reactive power of PMSG-WF. (c) DC-link voltage

quantities, PMSG rotor speed, and electromagnetic torque, respectively. The rotor speed is constant during a fault. Also, no oscillations are seen at the beginning and end of the fault for the electromagnetic torque graph.

Test 3: The third test studies the behavior of the PMSG-WF in response to 3LG fault on the utility grid. It is the worst condition during faults and requires the maximum support. The following figures illustrate the significant parameters of a PMSG-WT that are limited by the LVRT requirement. This requirement ensures the protection of the wind turbine components and allows for continued grid connection even at zero grid voltage. As seen in Fig.22a, the dynamics of the system are similar to the previous test (SLG and 2LG) faults. As

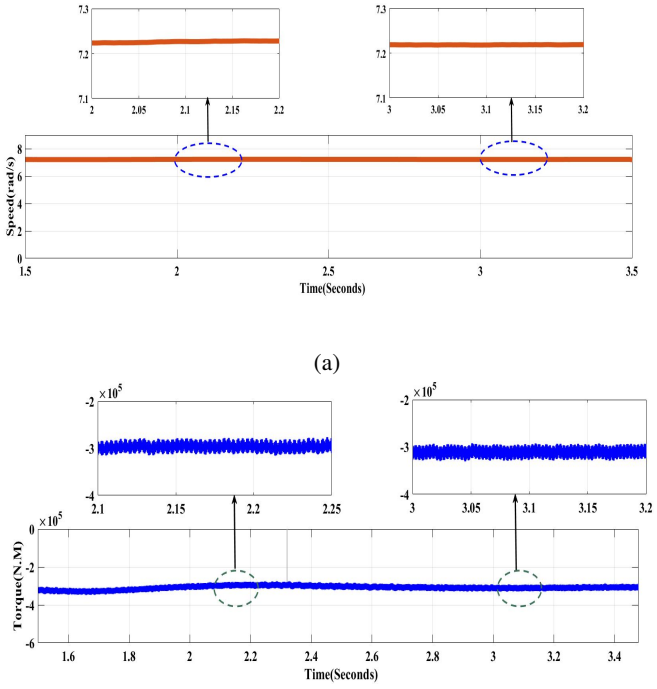

Fig. 18. (a) Rotor speed of PMSG (b)Electromagnetic torque of PMSG

shown in Fig.22b, the DVR instantly supplies the desired voltage and changes the voltage sag across the PCC from almost zero to its rated value,as seen in Fig.22c. This makes the PMSG-WF safer and especially improves its LVRT capabilities of wind generators.

In Fig.23a , Fig.23b and Fig.23c, the PMSG-WF current, PCC, active-reactive powers, and DC bus voltage are the different things that are shown. All these parameters exhibit small oscillations during fault onset and fault clearing, but they quickly return to their pre-fault values like nothing ever happened. Thanks to BC for saving the DC-link voltage constant and the DVR, which link PMSG-WF with the utility grid to compensate voltage at PCC during short-circuit fault. Fig.24a and Fig.24b show mechanical quantities for PMSG including rotor speed and electromagnetic torque. Again, there are no changes in these quantities.

B. The Comparison Between The Proposed System With Previous Works

In a previous work [26], a Static Shunt Var Compensator (SVC) was used to stabilize the grid voltage with disturbances on the WT and grid side under SLG and line-to-line faults.When a grid fault occurs, the SVC is automatically activated to regulate the grid voltage and compensate for the

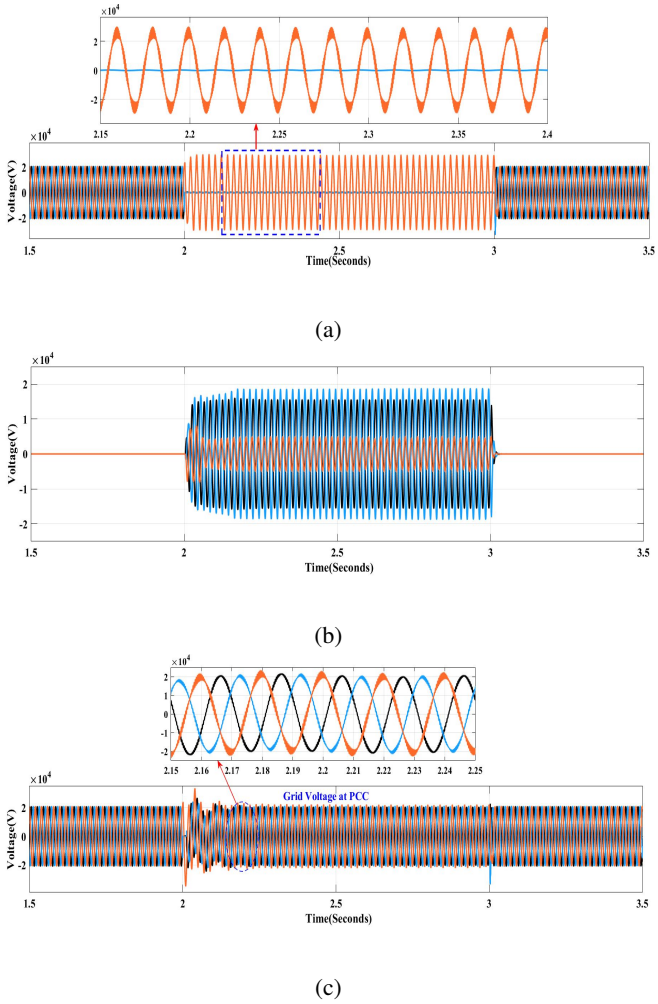

Fig. 19. Asymmetrical grid fault 2LG fault. (a) Grid voltage at B25 kV. (b) DVR compensation voltage. (c) PCC Voltage.

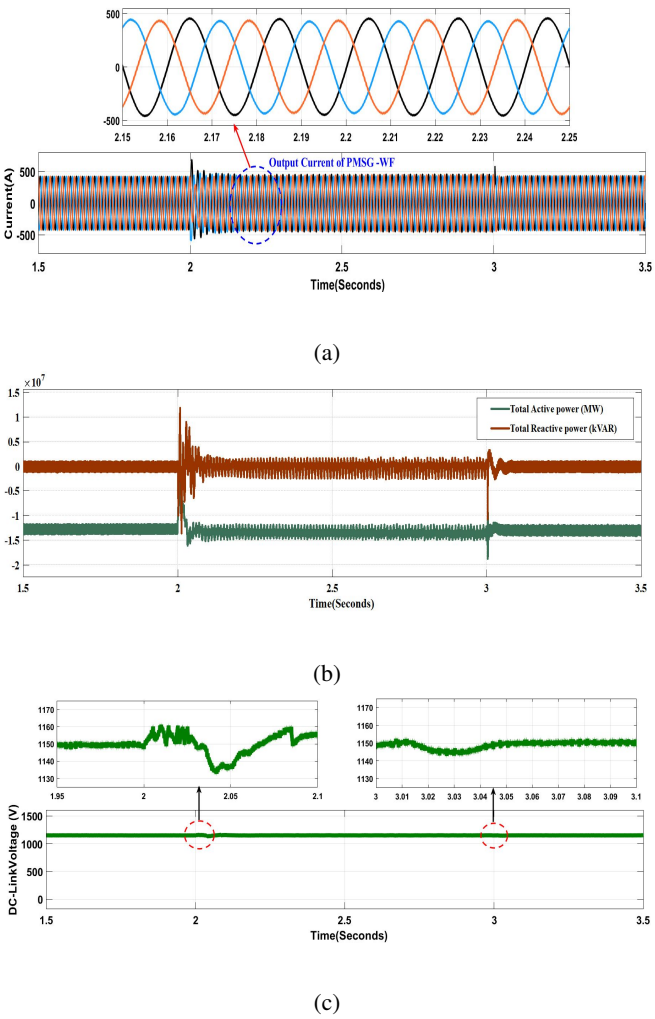

Fig. 20. (a) Output current of PMSG-WF (b) Reactive Power and Active Power of PMSG-WF. (c) DC-link voltage

power loss.The simulation results reveal that the voltage of the grid-integrated wind farm does not return to its original value during SLG fault with SVC, as evidenced by the simulation result of proposed system with DVR, which restored the PCC voltage to the pre-fault situation .Also in [2],the system includes a static synchronous compensator (STATCOM) and a BC connected to PMSG-WF to maintain stable operation during a three-phase symmetrical short-circuit fault.The simulation result for this system indicates that the speed and dc-link give higher overshoot and slower response in comparison to PMSG-WF outcomes using the proposed strategy during 3LG fault.So, DVR outperforms SVC and STATCOM by integrating into PMSG-WF to raise the voltage amplitude at PCC to its normal value during grid faults. It also prevents the PMSG-WF from encountering unacceptable transient voltages and currents while maintaining its conductivity during faults.

VI. Conclusion

In this paper, an FRT strategy for PMSG-WF is proposed.The proposed strategy uses a BC that is triggered, causing the excess active power to be dissipated in the resistance of the BC and keeping the DC-link voltage constant at its rated value (i.e., 1150 V).Also, the DVR has been used for reactive power compensation to supply controlled sinusoidal voltages in the face of voltage sags to maintain the PCC voltage of the PMSG-WF at the rated value during the faults, while the PMSG wind turbines continue its nominal operation.The simulation results under MATLAB/Simulink shows that DVR has superior performance in terms of compensation of the reactive power in severe disturbances,voltage stability,and

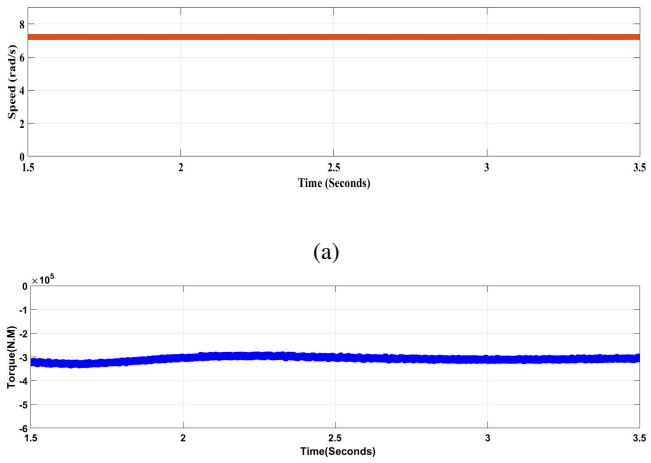

Fig. 21. (a) Rotor speed of PMSG (b)Electromagnetic torque of PMSG

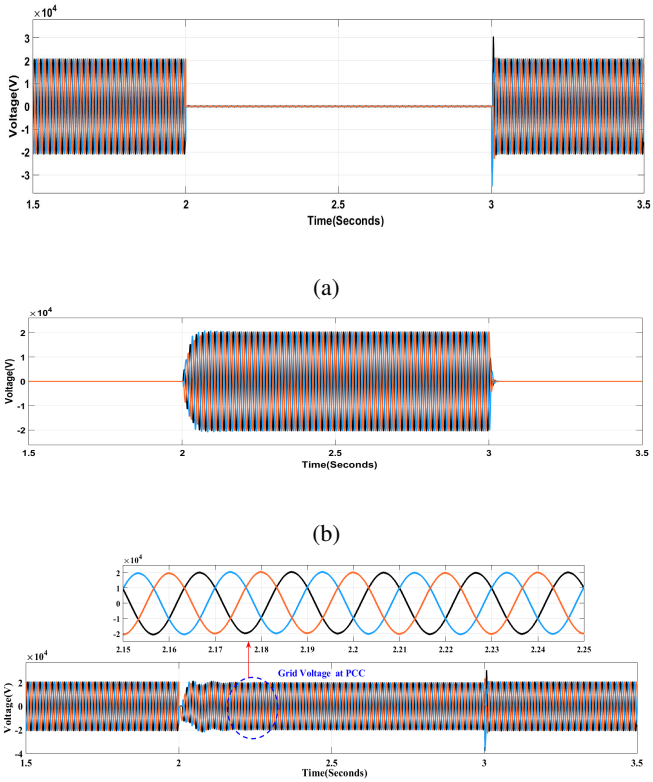

Fig. 22. Symmetrical grid fault 3LG fault. (a) Grid voltage at B25 kV. (b) DVR compensation voltage. (c) PCC Voltage .

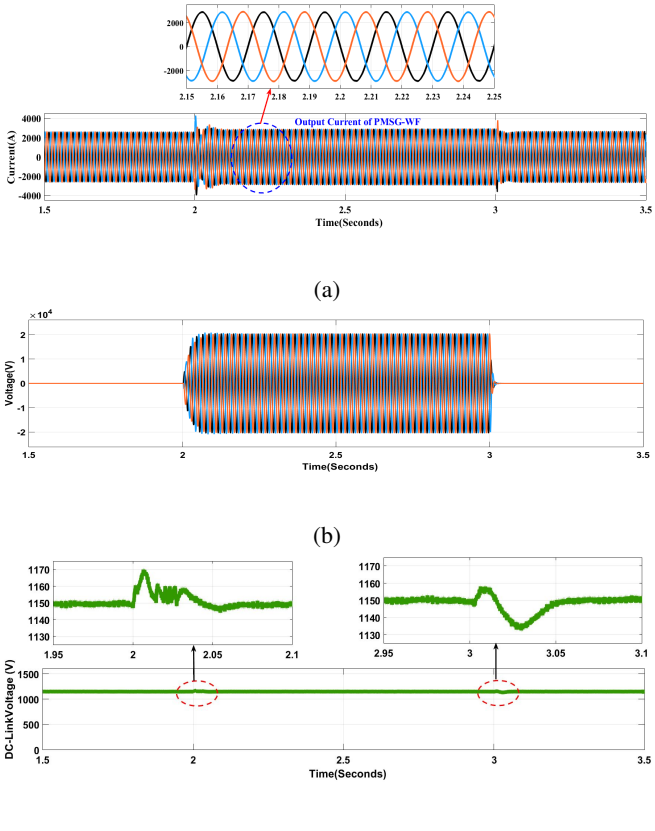

Fig. 23. (a) Output current of PMSG-WF (b)Reactive Power and Active Power of PMSG-WF. (c) DC-link voltage

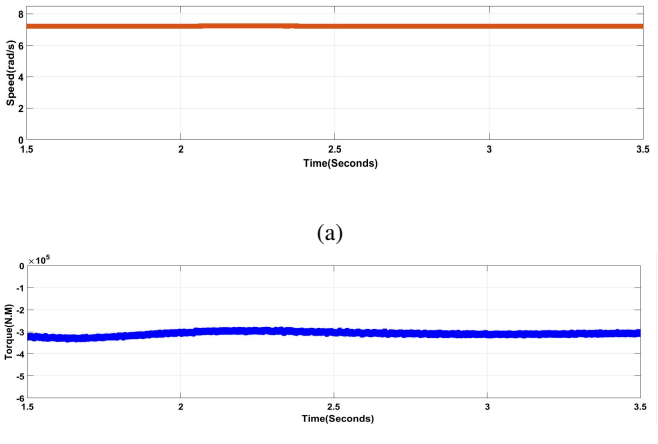

Fig. 24. (a) Rotor speed of PMSG (b)Electromagnetic torque of PMSG

power quality.Furthermore, the proposed system can recover

voltage quickly without suffering from voltage oscillation as experienced by other devices. Accordingly, the proposed FRT strategy fulfills the grid code requirements and shows the effectiveness of using a combination of BC and DVR with traditional PMSG-WF under various fault conditions.

CONFLICT OF INTEREST

The authors have no conflict of relevant interest to this article.

APPENDIX

Wind Turbine Parameters	
Parameters	Units
Rated power	2 MW
Air density	1.225 kg/m3
Radius of the swept area of blades	41 m
Rated wind speed	11.2 m/s
2 MW PMSG Parameters	
Rated stator voltage	690 V
Rated rotor speed	8.78 rad/s
Pole pairs	48
Stator resistance	$6*10^{-3}\Omega$
d-axis inductance	$0.3*10^{-3}H$
q-axis inductance	$0.3*10^{-3}H$
Stator resistance	$6*10^{-3}\Omega$
Transmission lines parameters	
Transformer ratio	690 V/25 kV
Rated frequency	50 Hz
Positive sequence resistance	0.1153Ω /m
Zero sequence resistance	$0.413\Omega/km$
Positive sequence inductance	0.00105 henries/km
Zero sequence inductance	0.00332 henries/km
Positive sequence capacitance	11.33e-9 farads/km
Zero sequence capacitance	5.01e-9 farads/km
DVR Parameters	
Inductance of VSI filter	6 mH
DVR DC voltage	45kV
Capacitance of VSI filter	1000 μF
Turns ratio of transformers	1
Source voltage(Grid) parameters	
Line to Line Voltage	120 kV
Supply frequency	50 Hz
3-phase short-circuit level	2500MVA

REFERENCES

[1] M. M. Mahmoud, B. S. Atia, Y. M. Esmail, M. Bajaj, D. E. Mbadjoun Wapet, M. K. Ratib, M. Biplob Hossain, K. M. AboRas, and A.-M. M. Abdel-Rahim, "Evaluation and comparison of different methods for improving fault ride-through capability in grid-tied permanent magnet synchronous wind generators," *International Transactions on Electrical Energy Systems*, vol. 2023, pp. 1–22, 2023.

[2] H. Geng, L. Liu, and R. Li, "Synchronization and reactive current support of pmsg-based wind farm during severe grid fault," *IEEE Transactions on Sustainable Energy*, vol. 9, no. 4, pp. 1596–1604, 2018.

[3] P. T. Nguyen, S. Stüdli, J. Braslavsky, and R. Middleton, "Coordinated control for low voltage ride through in pmsg wind turbines," *IFAC-PapersOnLine*, vol. 51, no. 28, pp. 672–677, 2018.

[4] H.-J. Lee, S.-H. Lim, and J.-C. Kim, "Application of a superconducting fault current limiter to enhance the low-voltage ride-through capability of wind turbine generators," *Energies*, vol. 12, no. 8, p. 1478, 2019.

[5] K. E. Okedu, M. Al Tobi, and S. Al Araimi, "Comparative study of the effects of machine parameters on dfig and pmsg variable speed wind turbines during grid fault," *Frontiers in Energy Research*, vol. 9, p. 681443, 2021.

[6] Y. Belkhier, T. Makhlouf, R. N. Shaw, A. Achour, and M. Bajaj, "Novel energy-based speed control of grid-connecting pmsg wind system," in *2021 IEEE 4th International Conference on Computing, Power and Communication Technologies (GUCON)*, pp. 1–6, IEEE, 2021.

[7] Y. Errami, A. Obbadi, and S. Sahnoun, "A survey of control strategies for grid connected wind energy conversion system based permanent magnet synchronous generator and fed by multi-level converters," *International Journal of Modelling, Identification and Control*, vol. 35, no. 1, pp. 51–63, 2020.

[8] L. Yuan, K. Meng, J. Huang, Z. Y. Dong, W. Zhang, and X. Xie, "Development of hvrt and lvrt control strategy for pmsg-based wind turbine generators," *Energies*, vol. 13, no. 20, p. 5442, 2020.

[9] M. Nasiri, J. Milimonfared, and S. Fathi, "A review of low-voltage ride-through enhancement methods for permanent magnet synchronous generator based wind turbines," *Renewable and Sustainable Energy Reviews*, vol. 47, pp. 399–415, 2015.

[10] K. Ma, M. Soltani, A. Hajizadeh, J. Zhu, and Z. Chen, "Wind farm power optimization and fault ride-through under inter-turn short-circuit fault," *Energies*, vol. 14, no. 11, p. 3072, 2021.

[11] X. Tian, P. Cheng, L. Wei, G. Li, H. Jiao, and H. Liu, "Transient stability and frt technologies of different synchronous wind turbine," *Energy Reports*, vol. 8, pp. 363–373, 2022.

[12] E. F. Morgan, O. Abdel-Rahim, T. F. Megahed, J. Suehiro, and S. M. Abdelkader, "Fault ride-through techniques for permanent magnet synchronous generator wind turbines (pmsg-wtgs): A systematic literature review," *Energies*, vol. 15, no. 23, p. 9116, 2022.

[13] M. Nasiri and A. Arzani, "Robust control scheme for the braking chopper of pmsg-based wind turbines–a comparative assessment," *International Journal of Electrical Power & Energy Systems*, vol. 134, p. 107322, 2022.

[14] B. Chandrika and B. Sujatha, "Voltage sag mitigation for pmsg system using dvr based hybrid fuzzy logic controller," in *Innovations in Electrical and Electronics Engineering: Proceedings of the 4th ICIEEE 2019*, pp. 503–513, Springer, 2020.

[15] P. K. Kesavan, U. Subramaniam, D. J. Almakhles, and S. Selvam, "Modelling and coordinated control of grid connected photovoltaic, wind turbine driven pmsg, and energy storage device for a hybrid dc/ac microgrid," *Protection and Control of Modern Power Systems*, vol. 9, no. 1, pp. 154–167, 2024.

[16] D. Pathak, S. Bhati, and P. Gaur, "Fractional-order nonlinear pid controller based maximum power extraction method for a direct-driven wind energy system," *International Transactions on Electrical Energy Systems*, vol. 30, no. 12, p. e12641, 2020.

[17] C. Kim and W. Kim, "Enhanced low-voltage ride-through coordinated control for pmsg wind turbines and energy storage systems considering pitch and inertia response," *IEEE Access*, vol. 8, pp. 212557–212567, 2020.

[18] M. Abdelrahem and R. Kennel, "Fault-ride through strategy for permanent-magnet synchronous generators in variable-speed wind turbines," *Energies*, vol. 9, no. 12, p. 1066, 2016.

[19] C. Kim and W. Kim, "Low-voltage ride-through coordinated control for pmsg wind turbines using de-loaded operation," *IEEE Access*, vol. 9, pp. 66599–66606, 2021.

[20] K. H.-M. Nguyen, Thai-Thanh and H. S. Yang, "Impacts of an lvrt control strategy of offshore wind farms on the hts power cable," *Energies*, vol. 13, no. 5, p. 1194, 2020.

[21] E. M. Boulaoutaq, A. Aziz, A. El Magri, A. Abbou, M. Ajaamoum, and A. Rachdy, "Low-voltage ride-through capability improvement of type-3 wind turbine through active disturbance rejection feedback control-based dynamic voltage restorer," *Clean Energy*, vol. 7, no. 5, pp. 1091–1109, 2023.

[22] A. Sedaghat, A. Hassanzadeh, J. Jamali, A. Mostafaeipour, and W.-H. Chen, "Determination of rated wind speed for maximum annual energy production of variable speed wind turbines," *Applied energy*, vol. 205, pp. 781–789, 2017.

[23] Z. Kang and J. Li, "Zero-voltage ride-through scheme of pmsg wind power system based on nleso and gftsmc," *Electronics*, vol. 12, no. 20, p. 4348, 2023.

[24] F. Hassanzadeh, H. Sangrody, A. Hajizadeh, and S. Akhlaghi, "Back-to-back converter control of grid-connected wind turbine to mitigate voltage drop caused by faults, conference: 49th north american power symposium, september 2017," 2017.

[25] N. Abas, S. Dilshad, A. Khalid, M. S. Saleem, and N. Khan, "Power quality improvement using dynamic voltage restorer," *IEEE Access*, vol. 8, pp. 164325–164339, 2020.

[26] S. A. Dayo, S. Memon, M. Uqaili, and Z. A. Memon, "Lvrt enhancement of a grid-tied pmsg-based wind farm using static var compensator," *Engineering, Technology & Applied Science Research*, vol. 11, no. 3, pp. 7146–7151, 2021.